analytical chemistry

pubs.acs.org/ac

Review

Signal Amplification by the *trans*-Cleavage Activity of CRISPR-Cas Systems: Kinetics and Performance

Wei Feng, Hongquan Zhang, and X. Chris Le*

Cite This: *Anal. Chem.* 2023, 95, 206−217

Read Online

ACCESS | Metrics & More | Article Recommendations

CONTENTS

Nucleic acid cleavage processes contribute to target and signal amplification, which is critical for the development of highly sensitive assays.[1,2] Exonucleases or endonucleases repetitively remove nucleic acid probes that bind to the target molecules and allow new probes to bind to the same target, achieving signal amplification.[3,4] Restriction endonucleases and nicking enzymes are often paired with polymerases to achieve linear or exponential amplification of target DNA.[5−7] DNAzymes can be specifically activated by a molecule or ion, and the multiple-turnover cleavage of their nucleic acid substrates results in signal amplification.[8−10] CRISPR (clustered regularly interspaced short palindromic repeats) systems have also been widely used for molecular detection because of the unique nuclease activities of CRISPR-associated (Cas) proteins.[11] A ribonucleoprotein (RNP), consisting of a Cas protein and a CRISPR RNA (crRNA) or single guide RNA (sgRNA), recognizes a target nucleic acid sequence. Binding of the target nucleic acid sequence to the RNP activates the enzyme.[12,13] Although often used for their sequence specificity in nucleic acid detection, the CRISPR-Cas systems have also been used for nucleic acid amplification or signal amplification.

The Cas9 RNP recognizes specific dsDNA and, with RuvC and HNH as two functional domains, it operates as an endonuclease to generate a staggered double-strand break.[12] Mutating one of the domains produces Cas9 nickase which cuts only one strand of dsDNA at a specific site. Such precise recognition and cleavage activities have been used for targeted amplification, and Cas9 nickase has been used as a nicking enzyme for exponential DNA amplification.[14,15]

The Cas12 RNP can recognize ssDNA and dsDNA with specific sequences. The hybridization between the target and crRNA activates Cas12, and with the RuvC domain, the active Cas12 cleaves the target (*cis*-cleavage) and nontarget ssDNA nearby (*trans*-cleavage).[16] The Cas13 RNP undergoes a conformational change upon binding to its ssRNA target, and then the HEPN1 and HEPN2 domains cleave any ssRNA indiscriminately.[17] The collateral cleavage of nontarget nucleic acids by active Cas12 and Cas13 systems is generally called *trans*-cleavage. With the unique *trans*-cleavage activity, Cas12 and Cas13 enzymes have been used for nucleic acid target recognition, signal generation, and amplification.[11,18,19] Upon activation by a target nucleic acid, Cas12 and Cas13 cleave short single-stranded reporter oligos through *trans*-cleavage, separating the fluorophore from the quencher which are typically labeled at opposite ends of the reporter molecule, and generating measurable fluorescence signals.

The *trans*-cleavage activity of Cas enzymes has been successfully used for signal amplification. One significant example is the detection of SARS-CoV-2 RNA without the need for traditional nucleic acid amplification.[20] The *trans*-cleavage process has also been used for the detection of non-nucleic acid targets that cannot be directly amplified.[21−23] When the CRISPR-Cas system is not coupled with other amplification techniques, the kinetics of *trans*-cleavage

Special Issue: Fundamental and Applied Reviews in Analytical Chemistry 2023

Published: January 10, 2023

https://doi.org/10.1021/acs.analchem.2c04555
Anal. Chem. 2023, 95, 206−217

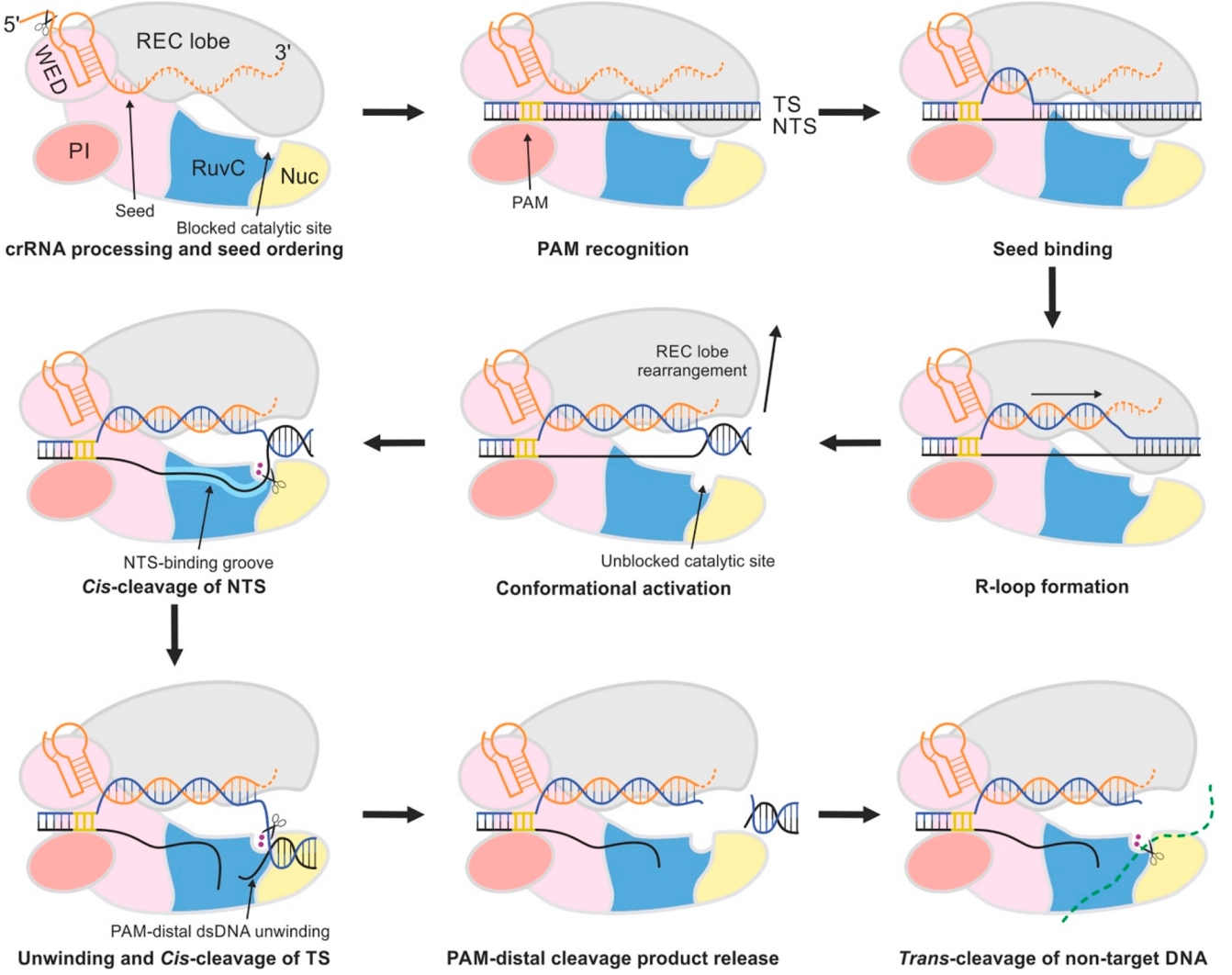

Figure 1. Mechanism of the nuclease activity of Cas12a.[44] FnCas12a is used as an example. Cas12a processes its crRNA by cleaving at the 5′ end of crRNA in microbes (step 1). Mature crRNA is often used for bioanalytical applications. PAM recognition is the first step of target recognition, which promotes the unwinding of dsDNA (step 2). The unwound target strand (TS) binds to the preordered seed region in crRNA (step 3). Further hybridization between crRNA and TS (step 4) forms the R-loop and induces a conformation change of Cas12a. The REC lobe moves away from the RuvC domain and unblocks the catalytic site (step 5). Active Cas12a then cleaves the target DNA (*cis*-cleavage), nontarget strand (NTS) (step 6), and then the TS (step 7). The PAM-distal product is released (step 8). The Cas12a ribonucleoprotein remains active as the PAM-proximal DNA fragment remains bound. With the same catalytic site, the active Cas12a cleaves indiscriminately any ssDNA (step 9, *trans*-cleavage). Note that the arrow in step 4 indicates the direction of "crRNA-TS hybridization" and concomitant "progressive target DNA duplex unwinding".[44] Reprinted with permission from Swarts, D. C.; Jinek, M. Mechanistic insights into the cis- and trans-acting DNase activities of Cas12a. *Molecular Cell* **2019** 73 (3), 589−600. Copyright 2018 Elsevier.

determines the signal amplification rate and thus the analytical sensitivity of CRISPR-based assays. Accurate characterization and improvement of the *trans*-cleavage kinetics are essential. Earlier reports of the kinetics of the *trans*-cleavage activity have overestimated activity because of calculation errors.[16,24−26] Ramachandran and Santiago[27] have promoted the correction of kinetics data. Although Chen et al.[16] initially reported a turnover number as high as 1250 s^{-1}, the authors later corrected the turnover number of LbCas12a to be 17 s^{-1}.[24] Subsequently, more kinetics data have been reported.[28,29] With accurately measured kinetics, we can estimate the limit of detection of assays that rely on Cas enzymes and understand factors that contribute to the kinetics.[27,29] Although *trans*-cleavage kinetics still limits the performance of CRISPR-based assays, efforts have been made to improve the kinetics and the overall performance of these assays.

In this review, we discuss the kinetics of the *trans*-cleavage activity and the signal amplification capability of CRISPR-Cas systems, especially Cas12 and Cas13 systems. By critically analyzing and comparing *trans*-cleavage kinetics data reported in the literature, we illustrate details of kinetics measurements and emphasize the importance of accurate measurements and correct calculations of *trans*-cleavage activities of Cas enzymes. The operation of Cas enzymes is a complicated process. Multiple factors affect *trans*-cleavage kinetics, but the detailed contribution of different factors has not been fully studied. We discuss the effects of Cas homologues, crRNA sequences, targets, reporters, cofactors, and other reaction conditions, all of which affect the *trans*-cleavage activity and kinetics. We limit

https://doi.org/10.1021/acs.analchem.2c04555
Anal. Chem. 2023, 95, 206−217

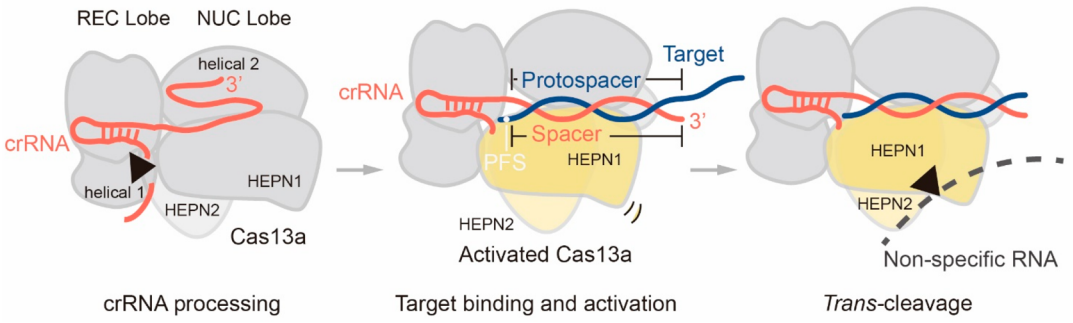

Figure 2. Mechanism of the ribonuclease activity of Cas13a. LbuCas13a is used as an example. Most Cas13a naturally process their own crRNA from the longer pre-crRNA (step 1), although in most applications, mature crRNA is synthesized *in vitro*. The crRNA-Cas13a complex binds to target RNA complementary to the spacer region within the crRNA (step 2), which activates Cas13a through a conformation change. The two HEPN domains move together and form a catalytic site (indicated with a black triangle in step 3). The HEPN domains cleave any RNA nearby indiscriminately, including the target RNA (*cis*-cleavage) or other nonspecific RNA substrates (*trans*-cleavage).

our discussion to assays that do not incorporate other amplification techniques so that we can prioritize various strategies to ensure high *trans*-cleavage activity and the overall performance of CRISPR-Cas-based signal amplification. While most reports focus on applications of *trans*-cleavage for nucleic acid detection *in vitro*, signal amplification in live cells has also been explored in the past year. Several challenges remain for both *in vitro* and *in vivo* applications of the *trans*-cleavage activity of CRISPR-Cas systems. We hope this review will promote the development of novel amplification strategies using the unique function of Cas nuclease and further improvements of assay performance.

FUNCTIONAL BASICS OF Cas12 AND Cas13

CRISPR-Cas12a (previously known as cpf1) and CRISPR-Cas13a (previously known as C2c2) systems are commonly used for molecular detection applications. The *trans*-cleavage (collateral cleavage) activity of Cas13 was discovered in 2016 and was used in nucleic acid detection soon after.[18,30,31] Cas12a was initially used for gene editing,[32] and after the discovery of its *trans*-cleavage activity,[16,33] it has been widely used for molecular sensing.[16,33] Here, we use Cas12a and Cas13a as examples to explain the basics and kinetics of the two types of Cas proteins. More Cas proteins with distinct features, such as Cas14[34−37] (Cas12f) and thermophilic Cas proteins,[38−40] have been discovered, characterized, and also used for nucleic acid detection. Three temperature-tolerant homologues, AacCas12b from *Alicyclobacillus acidoterrestris*,[38,41] AapCas12b from *Alicyclobacillus acidiphilus*,[39] and TccCas13a from *Thermoclostridium caenicola*,[40] have been used along with loop-mediated isothermal amplification (LAMP)[42] which operates at around 60 °C.

Nuclease Activity of Cas12a. Cas12a possesses three nuclease activities: endoribonuclease activity for crRNA processing, targeted nuclease activity on DNA strands (*cis*-cleavage), and nonspecific nuclease activity (*trans*-cleavage) toward ssDNA (Figure 1).[43,44] Cas12a has a molecular weight of approximately 150 kDa and a bilobed structure.[43,44] The only DNA-cleaving domain, RuvC, is located in the NUC lobe.[43,44] The direct repeat of crRNA, the 5′ stem-loop region, is recognized by the wedge domain (WED) of Cas12a.[44] Cas12a processes its crRNA by cleaving the 5′ end of the direct repeat.[45] For dsDNA, target binding starts with the recognition of the protospacer adjacent motif (PAM) by the WED and PI domains.[44] The canonical PAM is (T)TTV for LbCas12a, AsCas12a, and FnCas12a. The target strand (TS) and the nontarget strand (NTS) of the dsDNA are then unwound from the seed region.[44] The target strand hybridizes with the spacer of crRNA (∼20 nt), which allosterically activates Cas12a. The exposed catalytic site on the RuvC domain cleaves sequentially the unwound nontarget strand and then the target strand, generating sticky ends.[44] The cleavage of the target DNA is often referred to as *cis*-cleavage. The cleavage site is far from PAM, yet it may vary and be subject to postcleavage trimming.[46] The cleaved PAM-distal end of the ssDNA or dsDNA target is released from Cas12a while the PAM-proximal end of DNA remains bound.[46] After the cleavage of the target DNA, the RuvC domain cleaves nearby ssDNA indiscriminately. The latter process is referred to as *trans*-cleavage.[44] For ssDNA or unwound dsDNA targets, the PAM is not necessary.

Nuclease Activity of Cas13a. Cas13a operates as a ribonuclease. It processes its crRNA and can be activated by target ssRNA to nonspecifically cleave ssRNA (*trans*-cleavage) (Figure 2). For assay development, LbuCas13a from *Leptotrichia buccalis* and LwaCas13a from *Leptotrichia wadei* are most often used. Of these two homologues, LbuCas13a has more molecular architecture and mechanistic information available. LbuCas13a is a 138 kDa protein that contains a crRNA recognition (REC) lobe and a nuclease (NUC) lobe (Figure 2).[47] The primary RNA-cleaving domains are the two HEPN (higher eukaryotes and prokaryotes nucleotide-binding) domains located in the NUC lobe.[47] The direct repeat of crRNA (∼30−35 nt) is anchored in the REC lobe of Cas13a. Most Cas13a enzymes process their crRNA by cleaving at the 4 or 5 nucleotides upstream of direct repeat, the stem-loop region of crRNA.[48] crRNA processing is done by the HEPN2 domain and the helical 1 domain on the REC lobe of LbuCas13a.[48] The spacer of crRNA (20−30 nt) is located in the center of the NUC lobe (Figure 2). Nucleotides 9 to 15 interact extensively with LbuCas13a, and their bases are exposed to solvent.[47] These nucleotides may serve as a central seed region for target binding.[47,49] The hybridization between crRNA and target RNA induces a significant conformational change. Cas13a widens the central channel in the NUC lobe for the crRNA-target duplex, and the HEPN1 domain moves closer to the HEPN2 domain (Figure 2).[47] This brings catalytic residues on HEPN1 and HEPN2 together and activates Cas13a.[47] The active HEPN catalytic site of Cas13a cleaves exposed ssRNA indiscriminately. As the catalytic site of

https://doi.org/10.1021/acs.analchem.2c04555
Anal. Chem. 2023, 95, 206−217

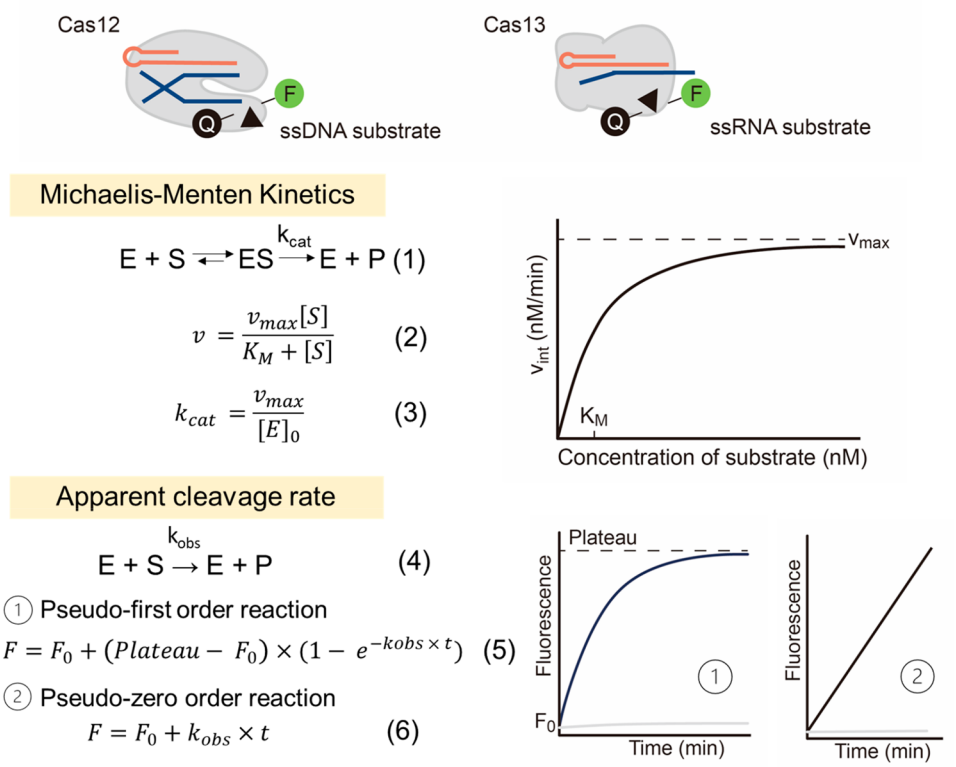

Figure 3. Description of Michaelis–Menten kinetics of the *trans*-cleavage activity of Cas12 and Cas13. The functional enzyme (E) of the *trans*-cleavage activity is the activated Cas12 or Cas13 ribonucleoprotein, and the enzyme concentration is the concentration of the ternary complex of Cas-crRNA-activator. The substrate (S) is the reporter, which is ssDNA for Cas12a and ssRNA for Cas13a. In the commonly used fluorescence measurement, the ssDNA or ssRNA reporter is labeled with a fluorophore (F) and a quencher (Q) at opposite ends of the short oligo. Products (P) of *trans*-cleavage are usually quantified by measuring fluorescence intensities. The Michaelis–Menten model delineates the inherent enzyme kinetics properties, including the catalytic rate constant or turnover number (k_{cat}), Michaelis constant (K_M), and catalytic efficiency (k_{cat}/K_M) (eqs 1–3). These kinetics properties can be obtained by measuring the reaction rates when using different concentrations of the substrate and a fixed concentration of the Cas-crRNA-activator ternary complex. Apparent cleavage rate (k_{obs}) can be obtained using the rate constant of either first-order reaction or zero-order reaction (eqs 4–6). The values of k_{obs} depend on experimental conditions.

LbuCas13a is away from the crRNA-target duplex, it may not cleave the protospacer of the target, the region hybridized with crRNA.[47]

QUANTITATIVE DETERMINATION OF *trans*-CLEAVAGE KINETICS OF Cas ENZYMES

The rate of *trans*-cleavage reactions can be best determined according to the Michaelis–Menten kinetics model (Figure 3). The enzyme for *trans*-cleavage is the ternary complex of Cas-crRNA-activator instead of either stand-alone Cas protein or crRNA-Cas ribonucleoprotein (RNP). Considering the potential dissociation of the ternary complex, a common strategy is to ensure much higher concentration of RNP than of the activator and the proper formation of the complex before use so that the activator concentration can be used as the approximate concentration of the ternary complex. Fluorescence systems are often used for the quantitative determination of *trans*-cleavage kinetics of Cas proteins. Nonspecific, short ssDNA or RNA substrates are labeled with a fluorophore (F) and a quencher (Q) at opposite ends, serving as quenched reporters (or probes). The *trans*-cleavage process cleaves the reporters and separates the quencher from the fluorophore, thereby generating fluorescence. Fluorescence intensity can be measured to quantify the amount of cleaved reporters (products). For quantitative determination and comparison of kinetics, the fluorescence intensity must be calibrated against standards and converted to the amount of substrate cleaved.[16,24]

Turnover numbers (k_{cat}) can be obtained using the Michaelis–Menten kinetics model (Figure 3). Michaelis–Menten kinetics considers the enzyme–substrate binding and the cleavage of substrates as two individual reactions (eqs 1–3). The turnover number (k_{cat}) is the maximum number of substrates cleaved by one activated Cas enzyme in one second if the amount of the substrate is in excess (unlimited). k_{cat} is calculated using eq 3. The maximum cleavage velocity (v_{max}) is obtained using eq 2 and by measuring the initial cleavage velocity (v_{int}) of reactions with a fixed concentration of enzyme ([E]) and varying concentrations of the substrate ([S]) (in excess).[16,24,27] Then k_{cat} is calculated by dividing the maximum velocity (v_{max}) by the fixed concentration of the enzyme ($[E]_0$). K_M represents the concentration of the substrate when the initial velocity (v_{int}) is half of the maximum velocity (v_{max}). k_{cat}/K_M is the catalytic efficiency, an overall measure of the efficiency of enzymatic conversion of the substrate to the product, involving both the rates of the enzyme–substrate binding and the cleavage process.

Noticing the errors and the overestimated turnover numbers previously reported by other researchers, Ramachandran and Santiago[27] established three back-of-the-envelope calculations to check the accuracy of the Michaelis–Menten kinetics parameters. First, for the calculation of v_{int}, the amount of the

https://doi.org/10.1021/acs.analchem.2c04555
Anal. Chem. 2023, 95, 206–217

Table 1. Summary of Michaelis–Menten Kinetics of Cas12 Homologues[a]

Ref.	Cas	crRNA	Activator	Reporter	k_{cat} (s^{-1})	K_M (nM)	k_{cat}/K_M ($M^{-1}s^{-1}$)
Chen et al. [16, 24]	LbCas 12a	-	ssDNA	DNaseAlert	3	620	5.0×10^6
			dsDNA		17	1010	1.7×10^7
Ramachandran et al. [27]	LbCas 12a	UAAUUUCUACUAAG UGUAGAUUGUAUGG CAUGAGUAACGAA	ssDNA	TTAT TATT	0.07	127	5.8×10^5
			dsDNA		0.09	213	4.2×10^5
		UAAUUUCUACUAAU GGUAGAUGUGGUAU UCUUGCUAGUUAC	ssRNA		0.09	96	8.9×10^5
			dsRNA		0.07	274	2.5×10^5
Nalefski et al. [28] *	LbCas 12a	UAAUUUCUACUAAG UGUAGAUCGCGCCA AAGCGACAGCCAC	dsDNA	F-C_{10}-Biotin	2.77	28	9.8×10^7
				F-C_{20}-Biotin	2.26	28	8.0×10^7
				DNaseAlert	1.30	26	5.1×10^7
				dsDNA	0.044	13	3.5×10^6
				F-rU_{20}-Biotin	0.118	133	8.9×10^5
			Long dsDNA (1299bp)	F-C_{10}-Biotin	1.32	49	2.7×10^7
		UAAUUUCUACUAAG UGUAGAUAGUAUUG CCUGUGUCGUCGG	dsDNA	F-C_{10}-Biotin	3.83	35	1.1×10^8
				F-C_{20}-Biotin	2.28	18	1.3×10^8
				DNaseAlert	1.02	23	4.4×10^7
				dsDNA	0.054	16	3.3×10^6
				F-rU_{20}-Biotin	0.338	108	3.2×10^6
Huyke et al. [29]	LbCas 12a	UAAUUUCUACUAAG UGUGAUGUGGUAUU CUUGCUAGUUAC	ssDNA1	TTAT TATT	0.58	310	1.9×10^6
			dsDNA1		0.38	370	1.0×10^6
		UAAUUUCUACUAAG UGUAGAUCCCCCAG CGCUUCAGCGUUC	ssDNA2		0.048	230	2.1×10^5
			dsDNA2		0.28	680	4.2×10^5
		UAAUUUCUACUAAG UGUAGAUAAUUACU UGGGUGUGACCCU	ssDNA3		0.29	240	1.2×10^6
			dsDNA3		0.19	320	5.9×10^5
		UAAUUUCUACUAAG UGUAGAUCUCAGGG CGGACUGGGUGCU	ssDNA4		0.27	180	1.4×10^6
			dsDNA4		0.32	260	1.2×10^6
		UAAUUUCUACUAAG UGUAGAUCCGCGGG UGGUCCCGGACAG	ssDNA5		0.098	120	8.5×10^5
			dsDNA5		0.078	82	9.5×10^5
		UAAUUUCUACUAAG UGUAGAUUGUAUGG CAUGAGUAACGAA	ssDNA6		0.30	260	1.2×10^6
			dsDNA6		0.56	490	1.1×10^6
		UAAUUUCUACUAAG UGUAGAUCGUCGCC GUCCAGCUCGACC	ssDNA7		0.022	450	4.9×10^4
			dsDNA7		0.028	870	3.3×10^4
Huyke et al. [29]	AsCas 12a	UAAUUUCUACUCUU GUAGAUCUGUGUUU AUCCGCUCACAA	dsDNA1	TTAT TATT	0.46	280	1.6×10^6
		GGUUUAAUUUCUAC UCUUGUAGAUCCGG CAAGCUGCCCGUGC CC	ssDNA2		1.3	420	3.0×10^6
			dsDNA2		0.90	1100	8.2×10^5
Huyke et al. [29]	Aap Cas12b	GUCUAGAGGACAGA AUUUUUCAACGGGU GUGCCAAUGGCCAC UUUCCAGGUGGCAA AGCCCGUUGAGCUU CUCAAAUCUGAGAA GUGGCACCGAAGAA CGCUGAAGCGCUG	ssDNA	TTAT TATT	0.13	660	2.0×10^5
			dsDNA		0.049	920	5.3×10^4
			ssDNA 60°C		0.16	1300	1.3×10^5
			dsDNA 60°C		0.12	1600	7.9×10^4
Rossetti et al. [51]	LbCas 12a	UAAUUUCUACUAAG UGUAGAUGUCUACA CAUGGCUAAAUCU	dsDNA	TTATT	0.30	250	1.2×10^6
				Stem-loop#5T **CTCTC***ATTTT TA***GAGAG**	0.24	42	6.1×10^6
				Stem-loop#10T	0.23	34	6.7×10^6
				Stem-loop#30T	0.28	69	4.1×10^6
Lv et al. [54]	LbCas 12a	-	-	-	0.43	584	7.4×10^5
Xie et al. [59]	LbCas 12a	UAAUUUCUACUAAG UGUAGAUGAUCGUU ACGCUAACUAUGA	dsDNA	TTATT	0.035	2051	1.7×10^4
					With additional Mn^{2+}		
					0.55	663	8.2×10^5

[a]The nucleotides in crRNA indicated with the lighter color represent the direct repeat sequence (the stem-loop region that binds to Cas). The nucleotides in crRNA indicated with the dark color denote spacers (the region that hybridizes with the target nucleic acid). *Most of the kinetics data in this paper were obtained using a magnetic beads–streptavidin–biotin substrate-capture platform.

https://doi.org/10.1021/acs.analchem.2c04555
Anal. Chem. 2023, 95, 206–217

Table 2. Summary of Michaelis–Menten Kinetics of Cas13 Homologues[a]

Ref.	Cas	crRNA	Target	Reporter	k_{cat} (s^{-1})	K_M (nM)	k_{cat}/K_M (M^{-1} s^{-1})
Slaymaker et al.[25-26]	PbuCas13b	-	ssRNA	U_6	0.95	-	-
Nalefski et al.[28]	LbuCas13a	Mature GGCCACCCCAAAAAUGAAGGGGACUAAAACGUGGGCGGUUGGUGUUA	ssRNA 1	F-U_5-Biotin	>3.3	>1000	3.3×10^6
				F-U_{10}-Biotin	>12	>1000	1.03×10^7
				F-U_{20}-Biotin	16.7	760	2.2×10^7
				RNaseAlert	27.1	294	9.2×10^7
		Mature GGCCACCCCAAAAAUGAAGGGGACUAAAACUACCUAGUCAUAGCCUCCGU	ssRNA 3	F-U_{10}-Biotin	320	2230	1.43×10^8
				F-U_{20}-Biotin	273	1500	1.82×10^8
				RNaseAlert	17.1	101	1.7×10^8
		Pre-crRNA GAUUUAGACCACCCCAAAAAUGAAGGGGACUAAAACGUGGGCGGCGGUUGGUGUUA	ssRNA 1	F-U_5-Biotin	164	2100	7.9×10^7
				F-U_{10}-Biotin	360	3400	1.1×10^8
				F-U_{20}-Biotin	290	1390	2.1×10^8
				RNaseAlert	25.8	330	7.8×10^7
		Pre-crRNA GAUUUAGACCACCCCAAAAAUGAAGGGGACUAAAACUACCUAGUCAUAGCCUCCGU	ssRNA 3	F-U_{10}-Biotin	740	3500	2.1×10^8
				F-U_{20}-Biotin	360	1100	3.2×10^8
				RNaseAlert	24.9	220	1.1×10^8
Huyke et al.[29]	LbuCas13a	GACCACCCCAAAAAUGAAGGGGACUAAAACGGUCCACCAAACGUAAUGCG	ssRNA 1	U_5	23	5800	4.0×10^6
		GACCACCCCAAAAAUGAAGGGGACUAAAACUUUGCGGCCAAUGUUUGUAA	ssRNA 2		11	5600	2.0×10^6
	LwaCas13a	GAUUUAGACUACCCCAAAAACGAAGGGGACUAAAACUGCUUCUGUCCAGUGAGCAUGGUCUCG	ssRNA 1		2.4	2100	1.2×10^6
		GAUUUAGACUACCCCAAAAACGAAGGGGACUAAAACACUCCCUAGAACCACGACAGUUUGCCUU	ssRNA 2		2.0	1800	1.1×10^6
Mahas et al.[40]	TccCas13a 56 °C	GUCACAACUCCCAUGUAGGCGGAGACUGCAACCCGAAGGUGUGACUUCCAUGCCAA	ssRNA	UGACGU	1.6	6660	0.24×10^6
Shinoda et al.[61] (~30 fL reaction)	LtrCas13a	GGAUUUAGAGUACCCCAAAAAUGAAGGGGACUAAAACAAGGUCUUCCUUGCCAUGUUGAGUGAGAGCGG	ssRNA N1	U_5	521	1540	3.4×10^8
		GGAUUUAGAGUACCCCAAAAAUGAAGGGGACUAAAACUUGGCAAUGUUGUUCCUUGAGGAAGUUGUAGC	ssRNA N2		457	1210	3.8×10^8
	LwaCas13a	GGAUUUAGACUACCCCAAAAACGAAGGGGACUAAAACAAGGUCUUCCUUGCCAUGUUGAGUGAGA	ssRNA N1	U_5	253	2040	1.2×10^8
		GGAUUUAGACUACCCCAAAAACGAAGGGGACUAAAACUUGGCAAUGUUGUUCCUUGAGGAAGUUG	ssRNA N2		192	1350	1.4×10^8
	LbuCas13a	GGACCACCCCAAAAAUGAAGGGGACUAAAACAAAGGUCUUCCUUGCCAUGUUGAGUGAGA	ssRNA N1	U_5	366	1260	2.9×10^8
		GGACCACCCCAAAAAUGAAGGGGACUAAAACAUUGGCAAUGUUGUUCCUUGAGGAAGUUG	ssRNA N2		596	2800	2.1×10^8

[a]The nucleotides in crRNA indicated with the lighter color represent the direct repeat sequence (the stem-loop region that binds to Cas). The nucleotides in crRNA indicated with the dark color denote spacers (the region that hybridizes with target RNA).

https://doi.org/10.1021/acs.analchem.2c04555
Anal. Chem. 2023, 95, 206−217

reporter cleaved ($v_{int}t_{lin}$) during the initial linear phase (t_{lin}) should not exceed the total amount of the reporter added before the reaction starts (S_0) (eq 7).[27] If the v_{int} has the wrong unit, e.g., arbitrary unit of fluorescence per second instead of nM per second, α would exceed 1, not meeting the criterion of eq 7.[27] Second, because v_{max} is calculated from the regression of eq 2, the measured reaction velocity (v), even when the substrate concentration [S] is high, should not exceed the v_{max} or $k_{cat}E_0$ (eq 8).[27] Third, the time scale of the linear phase (t_{lin}) should be at most on the same order of magnitude as the time scale (τ) at which the reaction completes.[27] If [S] $\ll K_M$, the time scale (τ) is close to $K_M/k_{cat}E_0$ (eq 9).[27] Although these three criteria are simple, many reported studies have not treated their kinetics data with this level of scrutiny.

$$\alpha = \frac{vt_{lin}}{S_0} < 1 \tag{7}$$

$$\beta = \frac{v}{v_{max}} = \frac{v}{k_{cat}E_0} \leq 1 \tag{8}$$

$$\gamma = \frac{t_{lin}}{\tau} = \frac{t_{lin}k_{cat}E_0}{K_M} \leq O(1) \tag{9}$$

The apparent cleavage rate (k_{obs}) is often measured (observed) from the entire cleavage process (eq 4) without separating the individual steps. k_{obs} values are useful for comparing many reaction designs under different experimental conditions. The fluorescence intensity either increases linearly with time or reaches a plateau, depending on the reaction conditions. When the concentration of the active Cas enzyme is much lower than that of the substrate, the initial phase of the fluorescence−time curve is linear, and the reaction is close to zero-order kinetics in which the apparent *trans*-cleavage rate (k_{obs}) is a constant (Figure 3 and eq 6).[50] When the substrate concentration is not much higher than that of the active Cas enzyme, the reaction is considered a pseudo-first-order reaction, and the reaction rate is k_{obs} multiplied by the substrate concentration ([S]). k_{obs} can be calculated using nonlinear regression of the fluorescence−time curve (Figure 3 and eq 5).[48,51] A measurement of k_{obs} requires only one substrate concentration. Therefore, the apparent cleavage rate (k_{obs}) is useful for large-scale kinetics comparisons of different enzymes under different conditions. However, the apparent cleavage rate varies with experimental conditions, such as the concentration of enzymes. Therefore, care should be exercised when comparing values of k_{obs} obtained under different experimental conditions.

■ *trans*-CLEAVAGE KINETICS OF Cas12 AND Cas13

The turnover number reflects the activity of the ternary target-crRNA-Cas complex. In addition to the Cas protein itself, the sequence of crRNA, choice of the target site, type of target, type of reporter,[28] reaction temperature,[29] cofactors,[32,52] inhibitors,[53] additives,[54] and even experimental procedures/operations[29] also affect the *trans*-cleavage activity. Thus, it is challenging to use a single kinetics number to define the activity of a Cas enzyme. Available Michaelis−Menten kinetics data are summarized in Tables 1 and 2. The listed studies meet the "back-of-the-envelope" check criteria[27] as described above. The turnover numbers provide general information on the magnitude of the signal amplification.

***trans*-Cleavage Kinetics of Cas12 and Its Contributing Factors.** Several groups have measured the kinetics of Cas12a homologues, and the reported k_{cat} ranges from 0.02 to 17 s^{-1} (Table 1).[16,24,27,28] Chen et al.[16,24] corrected their turnover number of LbCas12a from 1250 s^{-1} to 17 s^{-1}. The turnover number 1250 s^{-1} was incorrect because the fluorescence generation rate (arbitrary unit/s) was incorrectly used as the initial cleavage rate. The turnover number of a Cas12 homologue, AapCas12b, is 0.05−0.16 s^{-1}.[29] AapCas12b from *Alicyclobacillus acidiphilus* is a thermophilic Cas12 and has been used in the one-pot SHERLOCK assay for SARS-CoV-2 detection.[39] The turnover number of another homologue, AsCas12a, is 0.5−1.3 s^{-1}.[29] Because the reaction conditions used in these studies to obtain these turnover numbers are different, it is difficult to conclude which of the homologues has the highest activity.

Cas12a can be activated by different activators, which is an advantage of such an RNA-guided enzyme. However, the *trans*-cleavage activity induced by different activators and spacers varies. dsDNA and ssDNA may or may not induce different *trans*-cleavage activity for some crRNA (Table 1). Although using the same spacer design, Nalefski et al.[28] observed lower *trans*-cleavage activity when changing the activator from short targets to a longer target DNA. Huyke et al.[29] altered the nucleotide composition of the spacer and target DNA and reported up to a 20-fold change in the *trans*-cleavage activity of LbCas12a (Table 1). Engineering other components of crRNA, e.g., extension at the 5′ and 3′ end of crRNA, also contributes to a better *trans*-cleavage activity.[55]

Although the *trans*-cleavage of the ssDNA is nonspecific, LbCas12a prefers some reporters (substrates of nonspecific cleavage) over others. Commonly used reporters are short ssDNA (e.g., TTATT), poly C, and DNaseAlert, although the sequence of DNaseAlert is proprietary (Table 1). Lv et al.[54] compared the apparent cleavage rate when using 6-nt polyA, T, G, or C ssDNA as reporters and observed the highest cleavage rate when using cytosine-containing reporters. The cleavage rate was less than half when the poly A or poly T reporters were used, and there was very little cleavage of the poly G reporters.[54] The preference for cytosine was also reported by other groups.[28] Rossetti et al.[51] noticed that LbCas12a had a higher binding affinity (lower K_M) to longer reporters with stem-loop structures than to a 5-nt TTATT linear reporter (Table 1). The length of the reporter also affects the kinetics. The apparent cleavage rate of the 5-nt TTATT reporter was lower than that of the 8-nt linear reporter with a similar nucleotide composition[56] and at least 3-fold lower than that of the 10- and 20-nt linear reporter.[28] Poly C reporters of different lengths had a similar preference of 8-, 9-, and 10-nt spacers over a 5-nt spacer.[54]

Mg^{2+} is a common cofactor for the *trans*-cleavage activity of Cas enzymes and has been included in almost all relevant assays. Mg^{2+} also stabilizes crRNA folding[45] and enhances nucleic acid hybridization. Mn^{2+} also enhances the activity of Cas12 homologues (Table 1).[52,57−59] When used as a cofactor at the same concentration (10 mM), Mn^{2+} resulted in a higher LbCas12a activity than Mg^{2+}, and Mg^{2+} outperformed other divalent ions, Ca^{2+}, Cu^{2+}, Ni^{2+}, Co^{2+}, Ni^{2+}, Co^{2+}, Fe^{2+}, and Zn^{2+}.[57] A higher concentration of Mn^{2+} could further enhance the *trans*-cleavage kinetics of LbCas12a (Table 1).[59]

***trans*-Cleavage Kinetics of Cas13 and Its Contributing Factors.** *trans*-Cleavage kinetics of Cas13 varies with subtypes and homologues of Cas13. East-Seletsky et al.[48] compared the apparent cleavage rate of five Cas13a homologues, Lbu, Lwa, Ppr, Lba, and Hhe, using one

https://doi.org/10.1021/acs.analchem.2c04555
Anal. Chem. 2023, 95, 206−217

consistent set of spacers. They found that the LbuCas13a homologue had the highest *trans*-cleavage activity.[48] LbuCas13a generated measurable *trans*-cleavage activity in response to fM concentrations of ssRNA activator, followed by LwaCas13a which generated measurable signals in response to pM concentrations of activators.[48] The turnover number of Cas13 is generally over 1 s^{-1} (Table 2). Although Slaymaker et al.[25,26] initially reported a turnover number of 987 s^{-1} for PbuCas13b, the authors later corrected it to 0.95 s^{-1} (Table 2). Thermophilic TccCas13a has a reported turnover number of 1.6 s^{-1} (Table 2).[40]

Homologues within the Cas13a subtype have distinct features. Based on the nucleotide cleavage preference, Cas13a homologues can be grouped into two subfamilies: one group prefers uridine and the other prefers adenosine.[48] Lbu, Lwa, Lsh, and several other Cas13a homologues prefer uridine, whereas Lba, Era, and Cam homologues of Cas13a prefer adenosine.[48] Thus, poly U is a commonly used reporter for LbuCas13a and LwaCas13a. In addition, the *trans*-cleavage kinetics of LbuCas13a is faster for 10-nt and 20-nt poly U than for 5-nt poly U reporters.[28] Systematic studies of substrate preference have enabled the development of multiplex CRISPR assays.[60]

Both the spacer sequence (3′ end) and the 5′ sequence of crRNA affect the *trans*-cleavage rate. The difference in the *trans*-cleavage activity caused by the choice of the target site and the spacer design has been repeatedly observed (Table 2),[20,28,29] yet the underlying mechanism is not clear. A 5′ extension of the crRNA of Cas13a enhanced the *trans*-cleavage activity 10-fold (Table 2).[28] The 5′-extended crRNA is considered a precursor crRNA (pre-crRNA) and can be processed by Cas13a to become a shorter, mature crRNA.[28] However, the cleavage of the pre-crRNA is not a prerequisite for the activity enhancement, because even the Cas13a variant (K1082A) deficient in crRNA processing also showed enhanced activity when a pre-crRNA instead of a mature crRNA was used.[28]

The *trans*-cleavage activity is also significantly higher when the cleavage reaction takes place at the microscale.[61] The turnover numbers of three different Cas13a homologues reached 192−596 s^{-1} when the reactions took place in a ∼30 fL volume (Table 2).[61] Such kinetics is significantly higher than those when the reactions were conducted in larger (10−100 μL) volumes. There was no significant change in K_M (Table 2).[61]

NUCLEIC ACID DETECTION SENSITIVITY ACHIEVED BY *trans*-CLEAVAGE ACTIVITY OF Cas ENZYMES

Relations between the *trans*-Cleavage Kinetics and the Limit of Detection. The turnover number (k_{cat}) directly relates to the maximum signal amplification rate that can be achieved by CRISPR-Cas systems. The lower theoretical limit of detection can be estimated by dividing the concentration of the signal molecule required for a detector to give a positive signal by the maximum signal amplification fold within a certain time. The experimental limit of detection (LOD) cannot be lower than this theoretical limit. In practice, method LOD has been obtained by testing serially diluted targets. Using only Cas13a for signal amplification, researchers have reported successful detection of 10−1000 fM RNA (10^5−10^7 RNA molecules or copies) per reaction.[18,20] The analytical sensitivity and LOD are highly dependent on the choice of the target site/sequence.[18,20]

Huyke et al.[29] linked kinetics parameters with experimental LOD and reported the paired data for the target and crRNA listed in Tables 1 and 2. For the Cas12a crRNA-target pairs, the LOD agreed with the *trans*-cleavage kinetics.[29] LODs calculated on the basis of the slope of the fluorescence−time curve ranged from 0.21 to 130 pM, with a median of 2.9 pM.[29] The LOD calculated on the basis of the slope is lower than that of the end-point fluorescence measurement.[29] The LODs of different targets were consistent with the relative *trans*-cleavage kinetics responding to these targets. LODs of Cas13a-based assays were on the same order of magnitude as of Cas12-based assays, ranging from 1.1 to 82 pM.[29] There was a moderate correlation between catalytic efficiency (k_{cat}/K_M) and the LODs.[29]

Although introducing a nucleic acid amplification process is a common strategy for sensitive nucleic acid detection, techniques that rely solely on Cas systems for target recognition and signal amplification have been continually explored and improved. One of the strategies to improve the sensitivity of CRISPR-based assays is to enhance the *trans*-cleavage activity of Cas enzymes. In addition to optimizing the contributing factors of the *trans*-cleavage activities, as discussed above, an approach of using digital platforms to significantly reduce the reaction volume also enhances the kinetics.[61] Reactions in droplets or chip chambers with very small volumes[61−63] resulted in fast kinetics and high sensitivity.

Multiple Cas-crRNA RNPs have been used in parallel or in combination to form a positive-feedback cascade, resulting in a better assay performance. For example, pooled/combined crRNA improved the overall sensitivity of assays. Fozouni et al.[20] reported successful detection of 270 copies of SARS-CoV-2 RNA genome per μL and 100 copies of *in vitro* prepared partial genome per μL by targeting two well-chosen sites in the RNA at the same time and using a sensitive fluorescence detector. However, an initial nucleic acid amplification of the target RNA was required to achieve the sensitivity for detection of a few dozen copies of the target RNA per specimen.[64,65] Nalefski et al.[28] pooled 13 non-overlapped crRNA for Cas13a and achieved a 6- to 7-fold improvement of sensitivity. By pooling 20 crRNA for Cas12a, they achieved a detection limit of 310 aM. In another example, Shi et al.[66] built a feedback cascade with two Cas12a RNP. The activator for the first Cas12a RNP was target RNA. The guide RNA (gRNA) of the second Cas12a RNP was blocked by a bulge-containing ssDNA.[66] Cleavage of the bulge of the ssDNA released the ssDNA from the gRNA.[66] The artificial activator of the second RNP in the reaction activated Cas12a RNP2 to cleave the blocker and thus unblock gRNA2.[66] Fluorescence was generated by the process of blocker removal and cleavage of the bulge-containing ssDNA blocker that was dual-labeled with a fluorophore and a quencher.[66] Because gRNA2 or fluorescence blockers may not be 100% hybridized, maintaining high blocking efficiency and minimizing background fluorescence could be a challenge of such designs.

Nouri et al.[67] defined a figure of merit (FOM), the LOD multiplied by the reaction time (LOD × T), for the quantitative evaluation of CRISPR-based detection techniques (eq 10). Using the FOM, they also discussed how different factors improved assay performance, including improving the cleavage rate by each active Cas enzyme $\left(k_{cat}\frac{[S]}{K_M+[S]}\right)$, the

https://doi.org/10.1021/acs.analchem.2c04555
Anal. Chem. 2023, 95, 206−217

preamplification (A), high sample volume (V_0) over reaction volume (V_r) without affecting the assay, and low LOD of the detector (C_{min}) (eq 10).[67] Among different strategies they reviewed, digital-format assays, although without preamplification, resulted in FOMs that were closer to the techniques with nucleic acid amplification.[67]

$$\mathrm{FOM} = \mathrm{LOD} \times T = \frac{V_r C_{min}}{V_0 A k_{cat} \frac{[S]}{K_M + [S]}} \quad (10)$$

Prediction of Performance Aided by Machine Learning. The effect of sequence on Cas enzyme activity is complicated. Although some changes in crRNA or target sequence affect the kinetics, the effect may not apply to all targets. Beyond the *trans*-cleavage activity, other processes and factors contribute to the sensitivity and overall performance of a technique. Machine learning has enabled the prediction of the *cis*-cleavage activity of Cas9,[68] Cas12,[69,70] and Cas13[71,72] in live cells. These models were built on biochemical understanding of sequence preference and used principles of deep learning.[68] Predictions using deep learning required a large data set. High-throughput performance data of different gRNA were used for model development. For example, the authors used data from high-throughput sequencing and flow cytometry sorting after fluorescence protein editing.[69−72]

Although no universal rules are available for the choice of the target site within a long RNA for spacer design, deep neural networks have recently been explored to predict the performance of *in vitro* Cas13a assays. "ADAPT" (Activity-informed Design of All-inclusive Patrolling of Targets) is an automatic integrated tool for the design of crRNA to achieve good performance of CRISPR-based diagnostics.[73] ADAPT predicts crRNA that has a high diagnostic signal.[73] It also includes the analysis of related virus genomes to ensure the sensitivity and specificity of assays.[73] The activity data set for model development is from a high-throughput screen of over 19,000 crRNA-target pairs. Using a deep convolutional neural network model for their analysis, the authors showed a strong positive correlation between the predicted activity and the measured activity from the analysis of multiple test data sets (Spearman's correlation coefficient (ρ) of 0.7−0.8).[73]

The corresponding Cas13a activities of different crRNA-target pairs were measured using a microwell array platform, termed CARMEN (Combinatorial Arrayed Reactions for Multiplexed Evaluation of Nucleic acids).[65] In the CARMEN assay, different target molecules were dispersed into droplets, and so were the CRISPR reagent mixtures containing reporters and different crRNA for different nucleic acid targets. The identity of samples (amplicons) and crRNA were color-coded by controlling the ratio of four fluorophores that were added into the amplicon mix and the CRISPR reagent mix.[65] For each analysis on a chip that holds thousands of reactions, the droplets of the amplicon mixtures paired with the droplets of the CRISPR reagent mixtures, and each microwell held a random pair of droplets with one droplet from each mix.[65] The positive-or-negative signal generated from each microwell can be interpreted by using color-coding to identify the specific sample and the target within that microwell.[65]

CHALLENGES OF *trans*-CLEAVAGE AND SIGNAL AMPLIFICATION IN LIVE CELLS

Since the elucidation of the enzymatic activity of CRISPR-Cas9, CRISPR-Cas systems have been extensively used in live cells for editing and manipulation of genomes.[74] The *trans*-cleavage activity of Cas enzymes in live cells, especially in mammalian cells, has not been studied extensively. For Cas13, conflicting evidence has been reported.[75−77] If the *trans*-cleavage operates under intracellular conditions, introducing active Cas into live cells could collaterally damage ssDNA or ssRNA in the cells. Deactivated Cas9 (dCas9), dCas12, and dCas13 have been used for the imaging of nucleic acids in live cells.[19,78] The *trans*-cleavage-mediated signal amplification may further improve the sensitivity of molecular sensing in live cells.

The *trans*-cleavage activity of Cas12a has also been used for the sensing of non-nucleic acid targets.[79] The recognition of a non-nucleic acid target requires a transducer to bind the target molecule. The binding induces the formation, unlocking, or accumulation of the activator of Cas12 proteins.[21−23,80,81] Aptamers, DNAzymes, and antibodies that recognize and bind the target molecules or ions have been used as transducers.[19,21−23] These sensing applications have been demonstrated in test tubes. However, for signal amplification in live cells, intracellular conditions, the location and concentration of target molecules, and the delivery of probes and other reagents into the cells need to be considered.[82]

The signal amplification ability of Cas12a RNP in live cells has been explored. Chen et al.[83] introduced their Cas12a-based sensing platforms into cells. They designed dsDNA conditional probes for the sensing of miRNA, ATP, and telomerase in the cytoplasm. For telomerase sensing, the target strand of the dsDNA probe was shorter than the nontarget strand and served as a primer for telomerase to extend.[83] Telomerase extended the target strand and produced tandem telomeric repeats (AGGGTT). After extension, the dsDNA probe activated Cas12a. For ATP sensing, an ATP aptamer blocked half of the target strand of Cas12a.[83] Once bound to ATP, the aptamer released the target strand. The nontarget strand was initially hybridized to the other end of the target stand and then formed a dsDNA activator with the target strand. Similarly, the ssDNA blocker on the target strand was also designed to be complementary to the miRNA for its sensing.[83]

Different strategies have been developed to achieve high *trans*-cleavage activity and efficient delivery. Cofactors, such as Mg^{2+} and Mn^{2+}, are important for *trans*-cleavage activities. However, in live cells, the concentration of Mg^{2+} is generally lower than 1 mM.[84] This concentration of Mg^{2+} is insufficient for it to act as the cofactor for optimum *trans*-cleavage activity. Mn^{2+} has been used as a cofactor to enhance the *trans*-cleavage activity of Cas12a in live cells for molecular sensing.[58,59] Wang et al.[58] used MnO_2 nanosheet as a carrier and accelerator for Cas12a and achieved RNA sensing in live cells. Pan et al.[85] packaged ATP aptamers and CRISPR reagents in hollow covalent organic frameworks (COFs). COFs contributed to the internalization of the reaction reagents and served as a microreactor for CRISPR-Cas12a-mediated sensing.[85] As a small molecule, ATP entered the COF and was recognized by the ATP aptamer.[85] This binding released the ssDNA activator that was otherwise blocked by the ATP aptamer, which resulted in the activation of Cas12a and the generation of amplified signals.[85]

CONCLUDING REMARKS AND PERSPECTIVES

The *trans*-cleavage activity of CRISPR-Cas systems has been successfully used for signal amplification in molecular detection. The kinetics of *trans*-cleavage is critical to signal amplification efficiency. However, some miscalculated *trans*-

https://doi.org/10.1021/acs.analchem.2c04555
Anal. Chem. 2023, 95, 206−217

cleavage turnover numbers are still reported in the literature. We stress the importance of understanding the *trans*-cleavage kinetics of CRISPR-Cas systems. On the basis of the Michaelis−Menten kinetics model and critical evaluations of the reported kinetic data, we conclude that the *trans*-cleavage turnover number of Cas12 ranges from 0.02 to 17 s^{-1} and that of Cas13 ranges from 1 to 700 s^{-1}. These wide ranges of kinetic values are attributed to many factors that influence the activity and kinetics of *trans*-cleavage. Some of the most important factors include Cas homologues, crRNA sequences, targets, reporters, cofactors, reaction volumes, and other reaction conditions.

The primary application of *trans*-cleavage has been focused on nucleic acid detection in test tubes. The lower limit of detection is directly related to the *trans*-cleavage kinetics, such as turnover number (k_{cat}). A number of strategies have been explored to improve the *trans*-cleavage kinetics. One example is through testing various crRNA designs. In this regard, further studies are required to confirm whether the observed kinetics enhancement is universal to different target sequences. The molecular mechanisms behind the improvement are not clear. In addition to the *trans*-cleavage kinetics, the overall assay performance also depends on the kinetics of other processes such as target recognition. Details of other relevant processes are also important for the overall assay development. Machine learning has been used to predict the *trans*-cleavage activity and assay performance. The process requires large amounts of activity data of different sequences. Deep neural network models have shown promise for predicting activity, although a better mechanistic understanding would improve the accuracy of such predictions.

There have been recent attempts to use the *trans*-cleavage activity for signal amplification in live cells. Further understanding of the *trans*-cleavage activity of Cas enzymes in mammalian cells is needed. In addition to identifying whether there is *trans*-cleavage in live cells, it is also important to quantify the *trans*-cleavage activity and kinetics. Beyond the multiple factors that have been confirmed to impact the *trans*-cleavage activity in test tubes, the physiological conditions of live cells must be considered. For example, the likely lower concentrations of activators, delivery of reporters and/or substrates, the issue of accessibility, and the presence of potential inhibitors in the cells make it challenging for a controlled and efficient *trans*-cleavage in live cells. Further understanding of the kinetics of Cas systems in live cells can help minimize any unintended nonspecific cleavage, which is important for targeted editing and live cell sensing applications. In addition, new reporter and sensing designs are required to maintain reporting signals *in situ* for imaging applications.

AUTHOR INFORMATION

Corresponding Author

X. Chris Le − *Division of Analytical and Environmental Toxicology, Department of Laboratory Medicine and Pathology, Faculty of Medicine and Dentistry, University of Alberta, Edmonton, Alberta, Canada T6G 2G3;* orcid.org/0000-0002-7690-6701; Email: xc.le@ualberta.ca

Authors

Wei Feng − *Division of Analytical and Environmental Toxicology, Department of Laboratory Medicine and Pathology, Faculty of Medicine and Dentistry, University of Alberta, Edmonton, Alberta, Canada T6G 2G3;* orcid.org/0000-0003-1081-7914

Hongquan Zhang − *Division of Analytical and Environmental Toxicology, Department of Laboratory Medicine and Pathology, Faculty of Medicine and Dentistry, University of Alberta, Edmonton, Alberta, Canada T6G 2G3;* orcid.org/0000-0003-1088-9862

Complete contact information is available at: https://pubs.acs.org/10.1021/acs.analchem.2c04555

Notes

The authors declare no competing financial interest.

Biographies

Wei Feng is a postdoctoral fellow in the Department of Laboratory Medicine and Pathology at the University of Alberta (Canada). She obtained her B.Sc. in Biotechnology and M.Sc. in Biology, both from Beijing Institute of Technology, and Ph.D. in Analytical and Environmental Toxicology from the University of Alberta. Her research focuses on understanding and improving catalytic activities of CRISPR-Cas systems as well as developing bioanalytical assays for nucleic acids and proteins.

Hongquan Zhang is an Associate Professor in the Department of Laboratory Medicine and Pathology at the University of Alberta (Canada). He received his B.Sc. in 1997 and M.Sc. in 1999 from Northwest University (China) and Ph.D. in 2009 from the University of Alberta. He subsequently spent 3 years as a research associate in the Institute for Biological Sciences, National Research Council of Canada, and at the University of Alberta. His current research interests include (a) binding-induced DNA assembly and its applications to detection of proteins; (b) construction of binding-induced DNA nanomachines and nanodevices; and (c) generation, modification, and manipulation of functional nucleic acids.

X. Chris Le is Distinguished University Professor and Director of the Analytical and Environmental Toxicology Division in the Faculty of Medicine and Dentistry at the University of Alberta (Canada). He is also an adjunct professor in the Department of Chemistry and in the School of Public Health. He held the inaugural Canada Research Chair in Bioanalytical Technology and Environmental Health for 17 years. He is an elected Fellow of the Royal Society of Canada (Academy of Science) and Royal Society of Chemistry (U.K.). His interdisciplinary team develops ultrasensitive analytical techniques and studies human health effects from environmental exposure. His bioanalytical research focuses on the development of DNA−protein binding assays, isothermal and signal amplification techniques, CRISPR technology, fluorescence detection and imaging approaches, and targeted proteomics. His group uses these techniques to study DNA damage and repair, gene editing, DNA−protein interactions, arsenic-binding proteins, and environmental health.

ACKNOWLEDGMENTS

We thank the Natural Sciences and Engineering Research Council of Canada, the Canadian Institutes of Health Research, the New Frontiers in Research Fund, the Canada Research Chairs Program, Alberta Health, and Alberta Innovates for financial support. We thank our team members, including Jianyu Hu, Camille Huang, Teresa Kumblathan, Yanming Liu, Jeffrey Tao, Yiping Wu, Huyan Xiao, and JingYang Xu, for their comments and discussions, and Jeffrey Tao for creating the cover art.

REFERENCES

(1) Zhao, Y.; Chen, F.; Li, Q.; Wang, L.; Fan, C. *Chem. Rev.* **2015**, *115* (22), 12491−12545.
(2) Feng, W.; Newbigging, A. M.; Tao, J.; Cao, Y.; Peng, H.; Le, C.; Wu, J.; Pang, B.; Li, J.; Tyrrell, D. L.; Zhang, H.; Le, X. C. *Chem. Sci.* **2021**, *12* (13), 4683−4698.
(3) Zuo, X.; Xia, F.; Xiao, Y.; Plaxco, K. W. *J. Am. Chem. Soc.* **2010**, *132* (6), 1816−1818.
(4) Lu, C. H.; Li, J.; Lin, M. H.; Wang, Y. W.; Yang, H. H.; Chen, X.; Chen, G. N. *Angew. Chem., Int. Ed.* **2010**, *122* (45), 8632−8635.
(5) Walker, G. T.; Little, M. C.; Nadeau, J. G.; Shank, D. D. *Proc. Natl. Acad. Sci. U. S. A.* **1992**, *89* (1), 392−396.
(6) Walker, G. T.; Fraiser, M. S.; Schram, J. L.; Little, M. C.; Nadeau, J. G.; Malinowski, D. P. *Nucleic Acids Res.* **1992**, *20* (7), 1691−1696.
(7) Van Ness, J.; Van Ness, L. K.; Galas, D. J. *Proc. Natl. Acad. Sci. U. S. A.* **2003**, *100* (8), 4504−4509.
(8) Breaker, R. R.; Joyce, G. F. *Chem. Biol.* **1994**, *1* (4), 223−229.
(9) Li, J.; Lu, Y. *J. Am. Chem. Soc.* **2000**, *122* (42), 10466−10467.
(10) McConnell, E. M.; Cozma, I.; Mou, Q.; Brennan, J. D.; Lu, Y.; Li, Y. *Chem. Soc. Rev.* **2021**, *50* (16), 8954−8994.
(11) Abudayyeh, O. O.; Gootenberg, J. S. *Science* **2021**, *372* (6545), 914−915.
(12) Jinek, M.; Chylinski, K.; Fonfara, I.; Hauer, M.; Doudna, J. A.; Charpentier, E. *Science* **2012**, *337* (6096), 816−821.
(13) Knott, G. J.; Doudna, J. A. *Science* **2018**, *361* (6405), 866−869.
(14) Pardee, K.; Green, A. A.; Takahashi, M. K.; Braff, D.; Lambert, G.; Lee, J. W.; Ferrante, T.; Ma, D.; Donghia, N.; Fan, M.; Daringer, N. M.; Bosch, I.; Dudley, D. M.; O'Connor, D. H.; Gehrke, L.; Collins, J. J. *Cell* **2016**, *165* (5), 1255−1266.
(15) Wang, T.; Liu, Y.; Sun, H.-H.; Yin, B.-C.; Ye, B.-C. *Angew. Chem., Int. Ed.* **2019**, *58* (16), 5382−5386.
(16) Chen, J. S.; Ma, E. B.; Harrington, L. B.; Da Costa, M.; Tian, X. R.; Palefsky, J. M.; Doudna, J. A. *Science* **2018**, *360* (6387), 436−439.
(17) O'Connell, M. R. *J. Mol. Biol.* **2019**, *431* (1), 66−87.
(18) Gootenberg, J. S.; Abudayyeh, O. O.; Lee, J. W.; Essletzbichler, P.; Dy, A. J.; Joung, J.; Verdine, V.; Donghia, N.; Daringer, N. M.; Freije, C. A.; Myhrvold, C.; Bhattacharyya, R. P.; Livny, J.; Regev, A.; Koonin, E. V.; Hung, D. T.; Sabeti, P. C.; Collins, J. J.; Zhang, F. *Science* **2017**, *356* (6336), 438−442.
(19) Tang, Y.; Gao, L.; Feng, W.; Guo, C.; Yang, Q.; Li, F.; Le, X. C. *Chem. Soc. Rev.* **2021**, *50* (21), 11844−11869.
(20) Fozouni, P.; Son, S.; Diaz de Leon Derby, M.; Knott, G. J.; Gray, C. N.; D'Ambrosio, M. V.; Zhao, C.; Switz, N. A.; Kumar, G. R.; Stephens, S. I.; Boehm, D.; Tsou, C. L.; Shu, J.; Bhuiya, A.; Armstrong, M.; Harris, A. R.; Chen, P. Y.; Osterloh, J. M.; Meyer-Franke, A.; Joehnk, B.; Walcott, K.; Sil, A.; Langelier, C.; Pollard, K. S.; Crawford, E. D.; Puschnik, A. S.; Phelps, M.; Kistler, A.; DeRisi, J. L.; Doudna, J. A.; Fletcher, D. A.; Ott, M. *Cell* **2021**, *184* (2), 323−333.
(21) Xiong, Y.; Zhang, J.; Yang, Z.; Mou, Q.; Ma, Y.; Xiong, Y.; Lu, Y. *J. Am. Chem. Soc.* **2020**, *142* (1), 207−213.
(22) Dai, Y.; Somoza, R. A.; Wang, L.; Welter, J. F.; Li, Y.; Caplan, A. I.; Liu, C. C. *Angew. Chem., Int. Ed.* **2019**, *58* (48), 17399−17405.
(23) Li, Y.; Mansour, H.; Watson, C. J. F.; Tang, Y.; MacNeil, A. J.; Li, F. *Chem. Sci.* **2021**, *12* (6), 2133−2137.
(24) Chen, J. S. *Science* **2021**, *371* (6531), eabh0317.
(25) Slaymaker, I. M.; Mesa, P.; Kellner, M. J.; Kannan, S.; Brignole, E.; Koob, J.; Feliciano, P. R.; Stella, S.; Abudayyeh, O. O.; Gootenberg, J. S.; Strecker, J.; Montoya, G.; Zhang, F. *Cell rep.* **2019**, *26* (13), 3741−3751.
(26) Slaymaker, I. M.; Mesa, P.; Kellner, M. J.; Kannan, S.; Brignole, E.; Koob, J.; Feliciano, P. R.; Stella, S.; Abudayyeh, O. O.; Gootenberg, J. S.; Strecker, J.; Montoya, G.; Zhang, F. *Cell Rep.* **2021**, *34* (10), 108865.
(27) Ramachandran, A.; Santiago, J. G. *Anal. Chem.* **2021**, *93* (20), 7456−7464.
(28) Nalefski, E. A.; Patel, N.; Leung, P. J. Y.; Islam, Z.; Kooistra, R. M.; Parikh, I.; Marion, E.; Knott, G. J.; Doudna, J. A.; Le Ny, A.-L. M.; Madan, D. *iScience* **2021**, *24* (9), 102996.
(29) Huyke, D. A.; Ramachandran, A.; Bashkirov, V. I.; Kotseroglou, E. K.; Kotseroglou, T.; Santiago, J. G. *Anal. Chem.* **2022**, *94* (27), 9826−9834.
(30) East-Seletsky, A.; O'Connell, M. R.; Knight, S. C.; Burstein, D.; Cate, J. H.; Tjian, R.; Doudna, J. A. *Nature* **2016**, *538* (7624), 270−273.
(31) Abudayyeh, O. O.; Gootenberg, J. S.; Konermann, S.; Joung, J.; Slaymaker, I. M.; Cox, D. B.; Shmakov, S.; Makarova, K. S.; Semenova, E.; Minakhin, L.; Severinov, K.; Regev, A.; Lander, E. S.; Koonin, E. V.; Zhang, F. *Science* **2016**, *353* (6299), aaf5573.
(32) Zetsche, B.; Gootenberg, J. S.; Abudayyeh, O. O.; Slaymaker, I. M.; Makarova, K. S.; Essletzbichler, P.; Volz, S. E.; Joung, J.; van der Oost, J.; Regev, A.; Koonin, E. V.; Zhang, F. *Cell* **2015**, *163* (3), 759−771.
(33) Li, S.-Y.; Cheng, Q.-X.; Liu, J.-K.; Nie, X.-Q.; Zhao, G.-P.; Wang, J. *Cell Res.* **2018**, *28* (4), 491−493.
(34) Harrington, L. B.; Burstein, D.; Chen, J. S.; Paez-Espino, D.; Ma, E.; Witte, I. P.; Cofsky, J. C.; Kyrpides, N. C.; Banfield, J. F.; Doudna, J. A. *Science* **2018**, *362* (6416), 839−842.
(35) Wei, Y.; Yang, Z.; Zong, C.; Wang, B.; Ge, X.; Tan, X.; Liu, X.; Tao, Z.; Wang, P.; Ma, C.; Wan, Y.; Li, J. *Angew. Chem., Int. Ed.* **2021**, *60* (45), 24241−24247.
(36) Takeda, S. N.; Nakagawa, R.; Okazaki, S.; Hirano, H.; Kobayashi, K.; Kusakizako, T.; Nishizawa, T.; Yamashita, K.; Nishimasu, H.; Nureki, O. *Mol. Cell* **2021**, *81* (3), 558−570.
(37) Xiao, R.; Li, Z.; Wang, S.; Han, R.; Chang, L. *Nucleic Acids Res.* **2021**, *49* (7), 4120−4128.
(38) Li, L. X.; Li, S. Y.; Wu, N.; Wu, J. C.; Wang, G.; Zhao, G. P.; Wang, J. *ACS synth. Biol.* **2019**, *8* (10), 2228−2237.
(39) Joung, J.; Ladha, A.; Saito, M.; Kim, N.-G.; Woolley, A. E.; Segel, M.; Barretto, R. P. J.; Ranu, A.; Macrae, R. K.; Faure, G.; Ioannidi, E. I.; Krajeski, R. N.; Bruneau, R.; Huang, M.-L. W.; Yu, X. G.; Li, J. Z.; Walker, B. D.; Hung, D. T.; Greninger, A. L.; Jerome, K. R.; Gootenberg, J. S.; Abudayyeh, O. O.; Zhang, F. *N. Engl. J. Med.* **2020**, *383* (15), 1492−1494.
(40) Mahas, A.; Marsic, T.; Lopez-Portillo Masson, M.; Wang, Q.; Aman, R.; Zheng, C.; Ali, Z.; Alsanea, M.; Al-Qahtani, A.; Ghanem, B.; Alhamlan, F.; Mahfouz, M. *Proc. Natl. Acad. Sci. U. S. A.* **2022**, *119* (28), e2118260119.
(41) Yang, H.; Gao, P.; Rajashankar, K. R.; Patel, D. J. *Cell* **2016**, *167* (7), 1814−1828.
(42) Notomi, T.; Okayama, H.; Masubuchi, H.; Yonekawa, T.; Watanabe, K.; Amino, N.; Hase, T. *Nucleic Acids Res.* **2000**, *28* (12), 63e.
(43) Yamano, T.; Zetsche, B.; Ishitani, R.; Zhang, F.; Nishimasu, H.; Nureki, O. *Mol. Cell* **2017**, *67* (4), 633−645.
(44) Swarts, D. C.; Jinek, M. *Mol. Cell* **2019**, *73* (3), 589−600.e4.
(45) Swarts, D. C.; van der Oost, J.; Jinek, M. *Mol. Cell* **2017**, *66* (2), 221−233.e4.
(46) Strohkendl, I.; Saifuddin, F. A.; Rybarski, J. R.; Finkelstein, I. J.; Russell, R. *Mol. Cell* **2018**, *71* (5), 816−824.e3.
(47) Liu, L.; Li, X.; Ma, J.; Li, Z.; You, L.; Wang, J.; Wang, M.; Zhang, X.; Wang, Y. *Cell* **2017**, *170* (4), 714−726.
(48) East-Seletsky, A.; O'Connell, M. R.; Burstein, D.; Knott, G. J.; Doudna, J. A. *Mol. Cell* **2017**, *66* (3), 373−383.
(49) Tambe, A.; East-Seletsky, A.; Knott, G. J.; Doudna, J. A.; O'Connell, M. R. *Cell Rep.* **2018**, *24* (4), 1025−1036.
(50) Pang, B.; Xu, J.; Liu, Y.; Peng, H.; Feng, W.; Cao, Y.; Wu, J.; Xiao, H.; Pabbaraju, K.; Tipples, G.; Joyce, M. A.; Saffran, H. A.; Tyrrell, D. L.; Zhang, H.; Le, X. C. *Anal. Chem.* **2020**, *92* (24), 16204−16212.
(51) Rossetti, M.; Merlo, R.; Bagheri, N.; Moscone, D.; Valenti, A.; Saha, A.; Arantes, P. R.; Ippodrino, R.; Ricci, F.; Treglia, I.; Delibato, E.; van der Oost, J.; Palermo, G.; Perugino, G.; Porchetta, A. *Nucleic Acids Res.* **2022**, *50* (14), 8377−8391.

https://doi.org/10.1021/acs.analchem.2c04555
Anal. Chem. 2023, 95, 206−217

(52) Sundaresan, R.; Parameshwaran, H. P.; Yogesha, S.; Keilbarth, M. W.; Rajan, R. *Cell rep.* **2017**, *21* (13), 3728−3739.
(53) Knott, G. J.; Thornton, B. W.; Lobba, M. J.; Liu, J.-J.; Al-Shayeb, B.; Watters, K. E.; Doudna, J. A. *Nat. Struct. Mol. Biol.* **2019**, *26* (4), 315−321.
(54) Lv, H.; Wang, J.; Zhang, J.; Chen, Y.; Yin, L.; Jin, D.; Gu, D.; Zhao, H.; Xu, Y.; Wang, J. *Front. Microbiol.* **2021**, *12*, 766464.
(55) Nguyen, L. T.; Smith, B. M.; Jain, P. K. *Nat. Commun.* **2020**, *11* (1), 4906.
(56) Feng, W.; Peng, H.; Xu, J.; Liu, Y.; Pabbaraju, K.; Tipples, G.; Joyce, M. A.; Saffran, H. A.; Tyrrell, D. L.; Babiuk, S.; Zhang, H.; Le, X. C. *Anal. Chem.* **2021**, *93* (37), 12808−12816.
(57) Ma, P.; Meng, Q.; Sun, B.; Zhao, B.; Dang, L.; Zhong, M.; Liu, S.; Xu, H.; Mei, H.; Liu, J.; Chi, T.; Yang, G.; Liu, M.; Huang, X.; Wang, X. *Adv. Sci.* **2020**, *7* (20), 2001300.
(58) Wang, D.-X.; Wang, Y.-X.; Wang, J.; Ma, J.-Y.; Liu, B.; Tang, A.-N.; Kong, D.-M. *Chem. Sci.* **2022**, *13* (15), 4364−4371.
(59) Xie, S.; Xu, B.; Tang, R.; Chen, S.; Lei, C.; Nie, Z. *Anal. Chem.* **2022**, *94* (28), 10159−10167.
(60) Gootenberg, J. S.; Abudayyeh, O. O.; Kellner, M. J.; Joung, J.; Collins, J. J.; Zhang, F. *Science* **2018**, *360* (6387), 439−444.
(61) Shinoda, H.; Iida, T.; Makino, A.; Yoshimura, M.; Ishikawa, J.; Ando, J.; Murai, K.; Sugiyama, K.; Muramoto, Y.; Nakano, M.; Kiga, K.; Cui, L.; Nureki, O.; Takeuchi, H.; Noda, T.; Nishimasu, H.; Watanabe, R. *Commun. Biol.* **2022**, *5* (1), 473.
(62) Yue, H.; Shu, B.; Tian, T.; Xiong, E.; Huang, M.; Zhu, D.; Sun, J.; Liu, Q.; Wang, S.; Li, Y.; Zhou, X. *Nano Lett.* **2021**, *21* (11), 4643−4653.
(63) Tian, T.; Shu, B.; Jiang, Y.; Ye, M.; Liu, L.; Guo, Z.; Han, Z.; Wang, Z.; Zhou, X. *ACS Nano* **2021**, *15* (1), 1167−1178.
(64) Arizti-Sanz, J.; Freije, C. A.; Stanton, A. C.; Petros, B. A.; Boehm, C. K.; Siddiqui, S.; Shaw, B. M.; Adams, G.; Kosoko-Thoroddsen, T.-S. F.; Kemball, M. E.; Uwanibe, J. N.; Ajogbasile, F. V.; Eromon, P. E.; Gross, R.; Wronka, L.; Caviness, K.; Hensley, L. E.; Bergman, N. H.; MacInnis, B. L.; Happi, C. T.; Lemieux, J. E.; Sabeti, P. C.; Myhrvold, C. *Nat. Commun.* **2020**, *11* (1), 5921.
(65) Ackerman, C. M.; Myhrvold, C.; Thakku, S. G.; Freije, C. A.; Metsky, H. C.; Yang, D. K.; Ye, S. H.; Boehm, C. K.; Kosoko-Thoroddsen, T.-S. F.; Kehe, J.; Nguyen, T. G.; Carter, A.; Kulesa, A.; Barnes, J. R.; Dugan, V. G.; Hung, D. T.; Blainey, P. C.; Sabeti, P. C. *Nature* **2020**, *582* (7811), 277−282.
(66) Shi, K.; Xie, S.; Tian, R.; Wang, S.; Lu, Q.; Gao, D.; Lei, C.; Zhu, H.; Nie, Z. *Sci. Adv.* **2021**, *7* (5), eabc7802.
(67) Nouri, R.; Dong, M.; Politza, A. J.; Guan, W. *ACS Sens.* **2022**, *7* (3), 900−911.
(68) Konstantakos, V.; Nentidis, A.; Krithara, A.; Paliouras, G. *Nucleic Acids Res.* **2022**, *50* (7), 3616−3637.
(69) Kim, H. K.; Min, S.; Song, M.; Jung, S.; Choi, J. W.; Kim, Y.; Lee, S.; Yoon, S.; Kim, H. *Nat. Biotechnol.* **2018**, *36* (3), 239−241.
(70) Ameen, Z. S. i.; Ozsoz, M.; Mubarak, A. S.; Turjman, F. A.; Serte, S. *Alexandria Eng. J.* **2021**, *60* (4), 3501−3508.
(71) Wessels, H.-H.; Méndez-Mancilla, A.; Guo, X.; Legut, M.; Daniloski, Z.; Sanjana, N. E. *Nat. Biotechnol.* **2020**, *38*, 722−727.
(72) Guo, X.; Rahman, J. A.; Wessels, H.-H.; Méndez-Mancilla, A.; Haro, D.; Chen, X.; Sanjana, N. E. *Cell Genomics* **2021**, *1* (1), 100001.
(73) Metsky, H. C.; Welch, N. L.; Pillai, P. P.; Haradhvala, N. J.; Rumker, L.; Mantena, S.; Zhang, Y. B.; Yang, D. K.; Ackerman, C. M.; Weller, J.; Blainey, P. C.; Myhrvold, C.; Mitzenmacher, M.; Sabeti, P. C. *Nat. Biotechnol.* **2022**, *40* (7), 1123−1131.
(74) Adli, M. *Nat. Commun.* **2018**, *9* (1), 1911.
(75) Konermann, S.; Lotfy, P.; Brideau, N. J.; Oki, J.; Shokhirev, M. N.; Hsu, P. D. *Cell* **2018**, *173* (3), 665−676.e14.
(76) Abudayyeh, O. O.; Gootenberg, J. S.; Essletzbichler, P.; Han, S.; Joung, J.; Belanto, J. J.; Verdine, V.; Cox, D. B. T.; Kellner, M. J.; Regev, A.; Lander, E. S.; Voytas, D. F.; Ting, A. Y.; Zhang, F. *Nature* **2017**, *550* (7675), 280−284.
(77) Wang, Q.; Liu, X.; Zhou, J.; Yang, C.; Wang, G.; Tan, Y.; Wu, Y.; Zhang, S.; Yi, K.; Kang, C. *Adv. Sci.* **2019**, *6* (20), 1901299.
(78) Wu, X.; Mao, S.; Ying, Y.; Krueger, C. J.; Chen, A. K. *Genomics, Proteomics Bioinf.* **2019**, *17* (2), 119−128.
(79) Cheng, X.; Li, Y.; Kou, J.; Liao, D.; Zhang, W.; Yin, L.; Man, S.; Ma, L. *Biosens. Bioelectron.* **2022**, *215*, 114559.
(80) Shen, J.; Zhou, X.; Shan, Y.; Yue, H.; Huang, R.; Hu, J.; Xing, D. *Nat. Commun.* **2020**, *11* (1), 267.
(81) Li, Y.; Deng, F.; Hall, T.; Vesey, G.; Goldys, E. M. *Water Res.* **2021**, *203*, 117553.
(82) Peng, H. Y.; Newbigging, A. M.; Reid, M. S.; Uppal, J. S.; Xu, J. Y.; Zhang, H. Q.; Le, X. C. *Anal. Chem.* **2020**, *92* (1), 292−308.
(83) Chen, S.; Wang, R.; Peng, S.; Xie, S.; Lei, C.; Huang, Y.; Nie, Z. *Chem. Sci.* **2022**, *13* (7), 2011−2020.
(84) Grubbs, R. D. *Biometals* **2002**, *15* (3), 251−9.
(85) Pan, Y.; Luan, X.; Zeng, F.; Xu, Q.; Li, Z.; Gao, Y.; Liu, X.; Li, X.; Han, X.; Shen, J.; Song, Y. *Biosens. Bioelectron.* **2022**, *209*, 114239.

https://doi.org/10.1021/acs.analchem.2c04555
Anal. Chem. 2023, 95, 206−217